Is mild ADHD beneficial: Brain criticality is maximal with moderate ADHD symptom scores

Jonni Hirvonen[1,2,†], Hamed Haque[1,2,†], Sheng H. Wang[1], Jaana Simola[1,3], Isabel Morales-Muñoz[1,4,5], Benjamin U. Cowley[3,6], J. Matias Palva[1,7,8], Satu Palva[1,8]

[†]**These authors contributed equally to this work.**

Abstract

Attention-deficit/hyperactivity disorder (ADHD) is characterized by involuntary fluctuations of attention in continuous performance tasks (CPTs) wherein attention must be sustained over long periods of time. The neuronal basis underlying aberrant attentional fluctuations in time scales from seconds to minutes have remained poorly understood. Neuronal alpha- and gamma-band oscillations are thought to implement attentional and top-down control of sensorimotor processing. We hypothesized that aberrant behavioral fluctuations in ADHD would be caused by aberrant endogenous brain dynamics in alpha and gamma-band oscillations and specifically by their aberrant long-range temporal correlations (LRTCs). We measured brain activity with magnetoencephalography (MEG) from adult participants diagnosed with ADHD (N = 19) and from healthy control subjects (N = 20) during resting state and two CPTs; a threshold stimulus detection task and a Go/NoGo task. We then estimated LRTCs of neuronal oscillations and behavioral fluctuations with detrended fluctuation analysis (DFA). ADHD was associated with aberrant LRTCs in both behavioral performance and of neuronal oscillations. LRTCs were correlated with symptom severity with a U-shaped correlations indicating that the LRTCs were largest with moderate symptom scores. These data demonstrate the presence of aberrant temporal dynamics of neuronal oscillations in adult ADHD patients, which may underlie involuntary attentional fluctuations in ADHD. Taken that LRTCs are a hallmark of brain critical dynamics, these data show that moderate ADHD symptoms scores maximize brain criticality which is thought to be beneficial for performance.

Author affiliations:

[1] Neuroscience Center, Helsinki Institute of Life Science, University of Helsinki, Finland

[2] BioMag laboratory, HUS Medical Imaging Center, Finland

[3] Faculty of Educational Sciences, University of Helsinki, Finland

[4] Public Health and Welfare, Finnish Institute for Health and Welfare, Helsinki, Finland.

[5] Institute for Mental Health, School of Psychology, University of Birmingham, United Kingdom

[6] Cognitive Science, Department of Digital Humanities, Faculty of Arts, University of Helsinki

[7] Department of Neuroscience and Biomedical Engineering, Aalto University, Finland

[8] Centre for Cognitive Neuroimaging, Institute of Neuroscience and Psychology, University of Glasgow, United Kingdom

Correspondence should be addressed to:

Satu Palva

Neuroscience Center, Helsinki Institute of Life Science

Haartmaninkatu 3, P.O. Box 21

00014- University of Helsinki, Finland

satu.palva@helsinki.fi

Running Title: Aberrant scaling laws in adult ADHD

Keywords: ADHD; MEG; oscillation; criticality; long-range temporal correlations

Abbreviations: ADHD = Attention Deficit and Hyperactivity Disorder; ASRS = Adult ADHD Self-Report Scale; BADDS = Brown Attention Deficit Disorder Symptom Assessment Scale; BIS = Barrett Impulsiveness Scale; CPT = Continuous Performance Task; DAN = Dorsal Attention Network; DFA = Detrended Fluctuation Analysis; EOG =Electro-oculography; FA = False Alarm; FDR = False Discovery Rate; HR = Hit Rate; ICA = Independent Component Analysis; IQ = Intelligence quotient; lPFC = lateral Prefrontal Cortex; LRTC = Long-Range Temporal Correlation; MEG = Magnetoencephalography; mPFC = media Prefrontal Cortex; mPPC = medial Parietal Cortex; NE = Norepinephrine; PPC = Posterior Parietal Cortex; RS = resting state; RT = Reaction Time; RTV = Reaction Time Variability; SBM = Surface-based Morphometry; SOA = Stimulus Onset Asynchrony; TSDT = Threshold of Stimulus Detection Task; VAN = Ventral Attention Network

Introduction

Attention-deficit/hyperactivity disorder (ADHD) is a heritable neurodevelopmental condition that is characterized by detrimental levels of impulsive, inattentive and/or hyperactive traits.[1,2] ADHD affects 2.5–3.4 % of the adult population worldwide and its incidence has increased markedly in the last decade.[3] Current diagnostic tools for ADHD are largely based on subjective appraisals such as clinical interviews, self-reports, and observations by caregivers. However there are no reliable biomarkers that would enhance either the precision or accuracy of the diagnosis.[4] The development of reliable biomarkers and diagnostic criteria for ADHD are critically dependent on understanding the neuronal substrates of the disease symptoms, which may reveal ADHD-specific neuronal biotypes, or neurotypes, with abnormalities in neuronal dynamics despite no clear differences in behavioral testing.[5]

The cognitive functioning of individuals with ADHD is characterized by altered reaction times (RTs) and increased reaction time variability (RTV), which reflect the drifting of attention, loss of focusing, and failures in executive functions.[6–8] Such cognitive deficits are especially observable in excessive performance fluctuations in continuous performance tasks (CPTs) where attention must be sustained for a longer period of time in a monotonous or "boring" environment.[9,10] Elevated RTV and decreased response inhibition reflect individual differences in executive functioning and constitute an endophenotype in ADHD.[8] Attentional and executive functioning drifts involve time scales from seconds to hundreds of seconds in both healthy subjects and clinical populations. Behavioral performance in CPTs is characterized by slow oscillations or "streaks" in RT time-series,[8,11] and power-law long-range temporal correlations (LRTCs),[12,13] which are likely driven by similarly individually variable LRTCs in endogenous brain dynamics.[14] However, how behavioral LRTCs are associated with ADHD symptomatology or even how deficits in RTV and other psychophysical measures in ADHD patients are generally related to LRTCs have remained unclear.

Magnetic resonance imaging (MRI) of the brain has established that ADHD is associated with structural changes in surface-based morphometry (SBM) measures such as gyrification,[15] as well as with structural and functional connectivity[16] measures; albeit findings are somewhat inconsistent.[17] At the functional level, evidence for abnormal neuronal dynamics in ADHD patients have been found in electro- (EEG) and magnetoencephalography (MEG).[18–21] Alpha (8–12 Hz) and beta (13–30 Hz) band oscillations, which are fundamental for attention and top-down control,[21–26] show reduced task-dependent suppression and lateralization of local oscillation amplitudes in adults[21,27–29] and children[30] with ADHD. Such aberrant modulation of oscillation amplitudes are thought to arise from decreased structural connectivity (SC) between fronto-parietal (FP) regions.[28] However, even though these prior studies convergently indicate abnormal event-related and sub-second oscillation dynamics in ADHD, such short-range dynamics do not directly explain the temporally long-range and long time-scale deficits in sustained attention.

Oscillation amplitudes have been found to exhibit not only short-range correlations but also slow fluctuations over several seconds up to minutes. Similar to fluctuations in behavioral performance, these neuronal activity fluctuations are slowly decaying, scale-free (i.e. without characteristic temporal scale) and can be described with power-law LRTCs.[14,31–35] LRTCs are thought to be the hallmarks of brain criticality[36] and indicate that healthy brain activity is in the critical state between order and disorder that is thought to maximize the information processing capacity. Importantly, there are also large individual variability in neuronal LRTCs within healthy brain activity which predict variability of LRTCs in behavioral performance in CPT tasks and therefore predict the length of behavioral streaks in a trait-like manner.[11,14,33] Indicative of their critical role in healthy brain dynamics, LRTCs are attenuated in patients with epilepsy,[37] Alzheimer's disease,[38] schizophrenia or schizoaffective disorders,[39–41] autism spectrum disorder[42,43] and major depression,[44,45] compared to neurotypical control subjects. However, it remains unknown whether neuronal LRTCs are abnormal also in ADHD patients,

even though specifically this patient group struggles to sustain attention over long temporal durations and their behavioral performance is characterized by aberrant dynamics (e.g. increased RTV) especially in CPTs.

We tested here whether ADHD would be characterized by aberrant neuronal LRTCs by recording MEG data during two different CPTs from adult ADHD patients. We estimated behavioral LRTCs from the CPT RT time-series, and neuronal LRTCs from MEG oscillation amplitude fluctuations, using detrended fluctuation analysis (DFA). We found altered neural LRTCs in oscillation amplitude fluctuations in ADHD patients and demonstrated that they were correlated with both the variability in behavioral LRTCs and the severity of ADHD symptoms.

Methods and Materials

Participants

The sample comprised of N = 23 healthy neurotypical control participants (mean: 33 years old, range: 18-57; 15 females, 1 left-handed), and N = 23 patients with prior diagnosis of ADHD (mean: 36 years old, range: 26-59; 13 females, 3 left-handed) recruited from a previous study[46] and from the University of Helsinki students. The sample size was known to induce reliable LRTCs based on a previous study.[14] Inclusion criteria for all participants were: aged 18-60 years, male or female, normal or corrected to normal vision, and compatibility with MEG and MRI. Exclusion criteria included any substance abuse or medications active in the central nervous system and ADHD patients were asked to refrain from medications 24 hours before the MEG recordings. The control group exclusion criteria included any neurological or neuropsychiatric disorder and for the ADHD group any comorbid neurological or neuropsychiatric disorder or IQ < 80. This research was conducted in compliance with the

Declaration of Helsinki and approved by the Research Ethics Board at Helsinki University Central Hospital. All participants gave written informed consent prior to participation.

Psychopathology. The severity of ADHD in all participants was assessed with Barratt Impulsiveness Scale (BIS),[47] Brown Attention-Deficit Disorder Rating Scale (BADDS),[48] and Adult ADHD Self-Report Scale (ASRS)[49]; see Supplementary Table 1.

Tasks and Experiments

MEG data was collected during resting state (RS) activity and during two visual CPTs collected on separate days. Both tasks were presented in a projector screen inside a magnetically shielded room during MEG recordings.

Resting state. Eyes-open 10 min resting state MEG data, during which participants fixated at the fixation cross in the center of the screen, were collected before task data collection. Data for RS were collected from N = 23 control participant and N = 23 ADHD participants.

Visual Threshold of Stimulus Detection Task (TSDT). Participants were instructed to maintain fixation and detect the presence of stimuli presented at the visual threshold[14] and individually pre-calibrated to achieve a 50% detection rate using the adaptive QUEST algorithm (Supplementary Table 1).[50] Here misses reflect lapses in sustained attention. TSDT task was generated using Psychtoolbox-3. Visual stimuli of two shapes (50 % probability) were presented in any orientation with duration of 0.1 seconds in slowly-varying gradient noise with a diameter of 10° [51] and with a random stimulus onset asynchrony (SOA) of 1.5 – 4.5 s (Fig. 1A). During MEG, 500 stimulus trials were collected for each subject during a run of ~25 min.

Go/NoGo task. Go/NoGo task is as in,[12] where commission errors (i.e., erroneous responses to NoGo stimuli) constitute a measure of lack of sufficient cognitive control. The task was

coded using Presentation™ software (Neurobehavioral Systems, Inc., Albany, CA, USA). The stimulus was presented with a size of 1° for 0.1 s on a grey background with mean luminance of 107 cd/m^2 (Fig. 1B). The Go (75% of trials) and NoGo (25% of trials) stimuli were distributed randomly in the stimulus stream with SOA of 1 s.[12] Participants were instructed to respond as quickly as possible for the Go and withhold the responses for NoGo stimuli (Fig. 1B). A total of 1000 trials were collected for each participant.

Behavioral Data analysis

Detection Hit Rates (HRs) and Reaction times (RTs) for TDST were computed as the proportion of correct detection, with a response provided between 200–1500 ms from stimulus onset. Despite the calibration before experiments, HRs for participants varied and participants with HR < 25% were excluded from the analysis leaving N=19 ADHD and N=19 control subjects. HRs for the Go/NoGo task, were computed for the correctly responded Go-trials ('Hits') and incorrectly responded NoGo-trials ('Commission errors' i.e false alarms) for responses provided between 150–800 ms from the stimulus onset. Here, high HRs are indicative of successful task performance and HR < 70% for the Go stimuli were excluded leaving N=19 ADHD and N=20 control participants. Reaction time variability (RTV) was derived by computing standard deviations over the individual RTs in Go-trials. In the TSDT task, behavioral LRTCs were computed over the continuous sequence of Hit and Miss trials as in[14]. In the Go/NoGo task, RTs for Hits, and Commission Errors i.e. False Alarms (FA) were all included in the RT timeseries, as in[12]. LRTCs were then estimated from the RT time-series using Detrended Fluctuation Analysis (DFA) as in[52]. The scaling exponent β is a measure of temporal clustering such that higher β values indicate stronger temporal dependencies while values closer to 0.5 are associated with uncorrelated noise.

MEG and MRI Recordings

MEG data were recorded in the BioMag laboratory in HUS Medical Imaging Centre using 306-channel MEG (Elekta Neuromag TRIUX) with a sampling rate of 1000 Hz and online passband of 0.03-330 Hz. Electro-oculography (EOG) data were recorded to detect and then remove ocular artifacts. Behavioral responses were recorded with electromyography of abductor/flexor of pollicis brevis muscle and detected with an automatic algorithm. T1-weighted anatomical MRI scans for cortical surface reconstruction models were obtained for each subject at a resolution of 1 x 1 x 1 mm (MP-RAGE) with a 1.5-T MRI scanner (Siemens, Germany).

MEG preprocessing, source analysis, and surface parcellations

Source reconstruction and data analysis followed previously published procedures.[53–55] Maxfilter software (Elekta Neuromag) was used to suppress extra-cranial noise and interpolate bad channels. Independent component analysis (ICA) (MATLAB) was used for identifying and extracting ocular and heartbeat artefacts. The MEG data were Morlet-wavelet filtered between, f_{min} = 3 Hz … f_{max} = 148 Hz with m = 5. Freesurfer software was used for volumetric segmentation of the MRI data, surface reconstruction, flattening, and cortical parcellation/labeling with the Destrieux atlas. MNE software[56] was used for MEG-MRI co-localization, and preparation of the forward and inverse operators. Noise-covariance matrices (NCMs) were computed with a regularization constant of 0.05 using 200–250 Hz filtered baseline data (-0.75 - 0.25 s) for both TSDT and RS-data for the Go/NoGo task (4x1 min for NCM and 2x1 min for ADHD). Source-model dipoles had fixed orientation with 5 mm resolution. Source source-space vertices were collapsed into 400 cortical parcels using fidelity optimized parcellations[57] before further data-analysis.

Analysis of LRTCs from Neuronal MEG Data

To estimate the LRTCs of oscillation amplitude fluctuations, we applied DFA on the amplitude envelope of the Morlet-wavelet filtered parcel time-series signals[52] by segmenting data into time windows Δt from 1 to 225 seconds. Each segment of integrated data was then locally fitted similarly as for behavioral DFA.

Statistical analysis of behavioral data

Non-parametric Mann-Whitney U-test was used to test differences between the control and ADHD groups. The correlation between performance and the clinical total scores were assessed with Spearman's ranked correlation test. The correlation between behavioral DFAs and the clinical scores, and RTV in the Go/NoGo -task, were assessed with Spearman's ranked correlation test.

Statistical analysis of MEG data

Before statistical testing, the MEG data were collapsed into 200 parcels to decrease the impact of individual variability in brain functional anatomy. To identify the most significant and robust effects, statistical analyses were performed separately for each frequency and parcel. Within-group differences between task-state and resting-state activity were obtained with Wilcoxon signed-ranked test while group differences were obtained using Welch's *t*-test. The correlations between clinical scores and neuronal and behavioral scaling laws were estimated with Spearman rank correlation and quadratic correlations tests. Multiple comparisons were controlled with false discovery rate (FDR) correction at given the alpha-level (i.e., 5% at $\alpha = 0.05$). In addition, we applied a Q threshold to indicate the proportion of significant observations that could thereafter arise by chance in any of the wavelet frequencies. Only events that were above both corrected thresholds were considered significant.

Data availability statement

Anonymized data underlying figures will be made available upon publication.

Results

Clinical evaluations and Symptom data

We first validated that the ADHD participants had clinical symptoms as defined by ASRS, BIS, and BADDS scores, and that subjects in the control group had scores defined for neurotypical groups (Supplementary Table 1). For the ADHD group, the mean and standard deviation (SD) were 78.22 ± 12.88 for BIS, 67 ± 19.88 for BADDS, and 16.5 ± 3.68 ASRS (Fig. 1E). For the control participants, total scores were for ASRS were 8.79 ± 2.74 and for BIS were 59.58 ± 10.00, both of which were significantly lower than in the ADHD group (ASRS, Mann-Whitney U-test, p = 2.1E-7, BIS, Mann-Whitney U-test, p = 3.8E-5, Fig 1E). Although these symptom scores are not officially part of any diagnosis criterium for ADHD, be it ICD-10 or DSM-5, and have been used mostly for screening purposes or evaluating the response for treatments, it has been suggested that a total BIS sum of 72 or above should be used to classify an individual as highly impulsive.[58] In the case of ASRS, the maximum total score is 30, but for screening purposes certain questions weigh more than others. In this study, there were only two out of 23 control subjects who fulfilled these screening criteria. Taken together, these data show that ADHD symptoms in the control participants were mostly below or in the subclinical regime.

Behavioral task performance

We first assessed the classical behavioral measures of ADHD using TSDT (Fig. 1A) and Go/NoGo (Fig. 1B) tasks by estimating measures from the behavioral time-series data (Fig.

Fig. 1

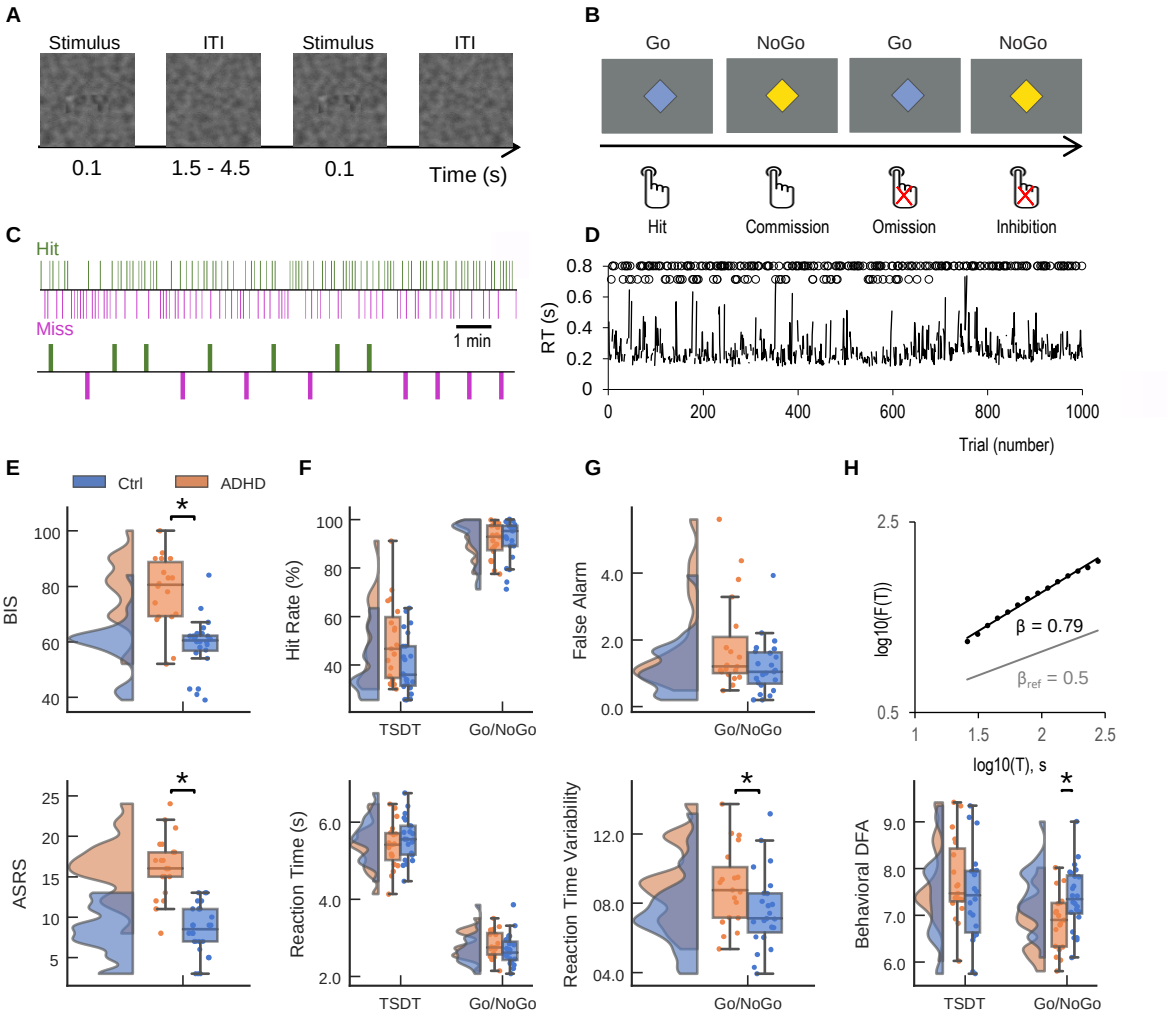

Figure 1. Task schematics and behavioral data. Schematics of (**A**) Threshold of Stimulus Detection Task (TSDT) and (**B**) Go/NoGo task experiments. (**C**) A short snapshot period of Hit-Miss time-series of a representative subject in TSDT. (**D**) Reaction Time (RT) series of a representative subject for each trial in Go/NoGo. Circles in the lower line above the time-series represent commission errors and circles in the upper line are trials with successful inhibition. (**E**) Distribution of BIS and ASRS scores for N = 21 ADHD patients (orange) and N = 23 neurotypical control (blue) subjects. (**F**) Distribution of Hit rate (HR), and RT distributions separately for TSDT and Go/NoGo tasks. (**G**) False Alarm (FA) rate and Reaction Time Variability (RTV). (**H**) Behavioral DFA (Detrended Fluctuation Analysis) exponents for a representative subject (top) and for the Ctrl and ADHD groups (bottom). Figure displays subject means ± 25 % for each psychophysical parameter. The parenthesis above the figure illustrates significant difference between the groups for the RTs (two-tailed Mann-Whitney U-test (U = 132), $p = 0.043$)) and RTVs (two-tailed Mann-Whitney U-test, $p = 0.012$).

1C-D). Taken that the TSDT task performance was pre-calibrated to a 50% stimulus-detection rate (Hit Rate, HR), as expected, the between-group differences in HRs were not significant for TSDT (Fig. 1F) (Control group (Ctrl) 40.35 ± 11.76 % (mean ± SD), ADHD patients 49.45 ± 16.24%, Mann-Whitney U-test, $p = 0.087$) nor were there differences in reaction times (RTs) (Ctrl 0.56 ± 0.0455 s, ADHD 0.54 ± 0.058 s, Mann-Whitney U-test, $p = 0.26$). In the Go/NoGo task, HRs (Ctrl 91.5 ± 8.31 %, ADHD 91.27 ± 6.86 %, Mann-Whitney U-test, $p = 0.77$) nor RTs (Control 0.27 ± 0.039 s, ADHD 0.28 ± 0.035 ms, Mann-Whitney U-test, $p = 0.14$) were significantly different between the groups neither were the False alarms (FA) (Fig 1 E) (Ctrl 0.12 ± 0.08 %, ADHD patients 0.18 ± 0.14 %, Mann-Whitney U-test, $p = 0.14$, Fig. 1G). However, as found previously, the reaction time variability (RTV) was larger for the ADHD group compared to the control group (Ctrl 0.076 s ± 0.022, ADHD patients 0.089 s ± 0.022, Mann-Whitney U-test, $p = 0.038$, Fig. 1G).

We then identified long-range temporal correlations (LRTCs), or “streaks”, in behavioral Hit Miss times-series (Fig. 1C) and RT time-series (Fig. 1D) data for the TSDT and Go/NoGo tasks, respectively, by using DFA (Fig 1H). DFA exponents did not differ between control and ADHD groups for TSDT (0.74 ± 0.095 and 0.78 ± 0.086 respectively, Mann-Whitney U-test, $p = 0.34$, Fig 1H), but in the Go/NoGo task, DFA exponents were larger in the control than in the ADHD group (0.74 ± 0.066 in the control group and 0.69 ± 0.06 in the ADHD group, Mann-Whitney U-test, $p = 0.018$).

Neuronal LRTCs differ between ADHD and control groups

Oscillation amplitude envelopes were extracted from Morlet-wavelet filtered time-series of source-reconstructed MEG data (Fig. 2A) and used detrended fluctuation analysis (DFA) to identify DFA exponents (Fig. 2B). We first conducted a whole-brain-level analysis of neuronal LRTCs from oscillation amplitude envelopes such that the neuronal DFA scaling exponents

Fig. 2

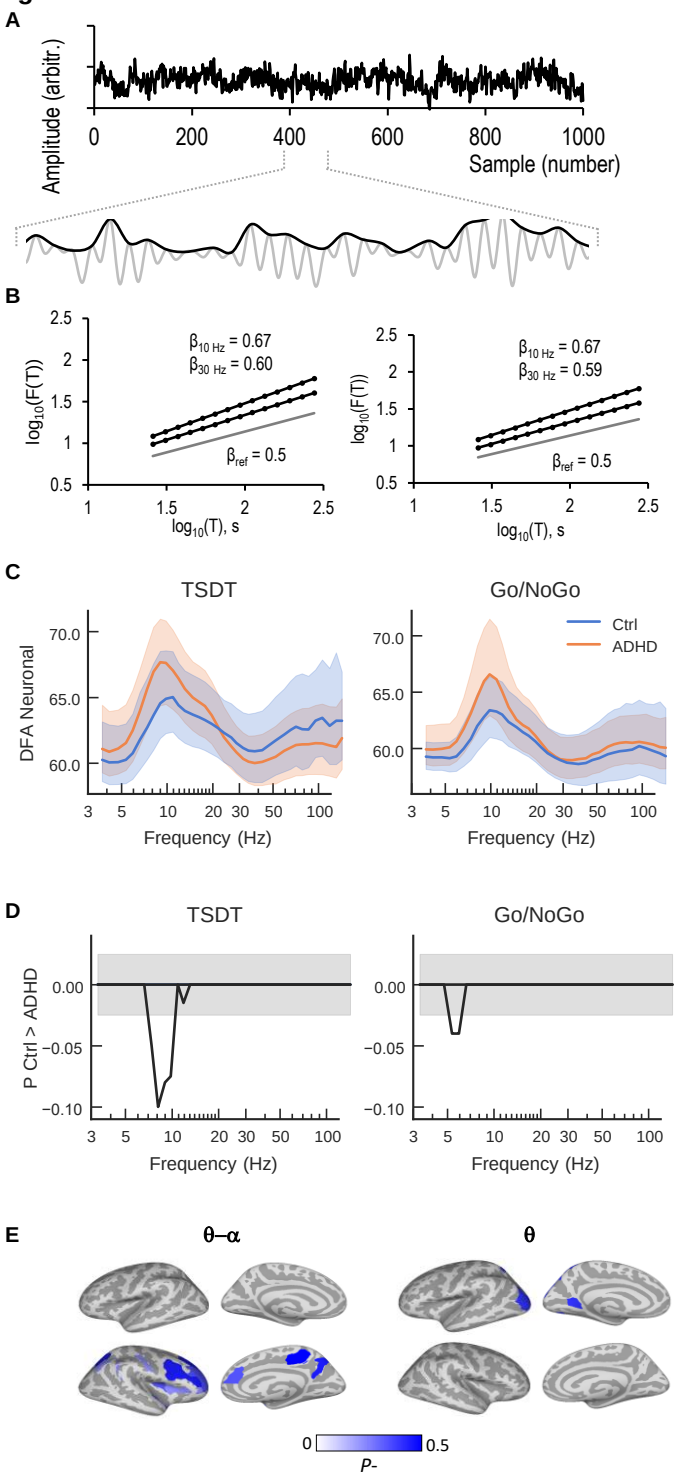

Figure 2. Differential modulations of neuronal DFA exponents in ADHD and control groups at the whole-brain level. (**A**) Example of unfiltered neuronal time-series (top) and filtered oscillation amplitude time-series (bottom, gray trace) with the amplitude envelope (bottom, black trace) (**B**) DFA exponents extracted from oscillation amplitude envelope for a representative subject. (**C**) Group-level mean DFA -exponents averaged over all parcels as a function of frequency for ADHD (orange) and control (blue) groups during TSDT (Threshold of Stimulus Detection Task) and Go/NoGo tasks. Lines above indicate significant differences between the groups. Gray shading shows 95% confidence intervals. (**D**) Group-level differences in the DFA exponents between control and ADHD groups estimated separately for each cortical parcel (Welch *t*-test, $p < 0.05$, FDR corrected). The *y*-axis shows the fraction of cortical parcels (*P*) in which the difference was significant. Grey lines indicate Q -level of 0.025 for 95th percentile for FDR correction indicating the proportion that could arise by change. (**E**) Cortical regions in which the differences in theta/alpha (θ-α, 6-13 Hz) were observed in TSDT and in theta (θ) -band (5-8 Hz) DFA exponents were observed. The blue color indicates the fraction of time-frequency elements (*P*-) that were significantly suppressed and red the fraction of time-frequency elements (*P*+) that were significantly increased.

were computed across all parcels for the task. The whole-brain mean DFAs averaged across all parcels (brain areas) peaked in the alpha-band (α, 8–13 Hz) in both tasks (Fig. 2C).

To assess the group differences at parcel-level anatomical resolution, we computed parcel-wise differences in LRTCs between the groups. In line with the whole-brain-average analysis, the DFA exponents were smaller for control than for the ADHD group in the theta-alpha (θ–α, 6-10 Hz) band in the TSDT task and in the low theta (θ, 3–4 Hz) band in the Go/NoGo task (Fig. 2D) (Welch's *t*- test, $p < 0.05$, FDR corrected). Stronger LRTCs of theta-alpha oscillations in ADHD patients than in control participants were found in the occipital cortex in both tasks and during the TSDT task additionally in posterior parietal cortex (PPC) and temporal cortex (Fig. 2E).

Different task-dependent modulation of LRTCs in ADHD patients

We then asked in parcel-level resolution whether these differential task effects between groups on LRTCs would be caused by different task dependent modulation compared to rest within the groups. In the control group, the theta-alpha (θ–α, 6-13 Hz) band DFA scaling exponents were suppressed in the task conditions compared to the in resting-state (RS) and increased from the RS in the wide gamma-band (γ, 30–60 Hz) (Fig. 3A) (Wilcoxon signed rank test, $p < 0.05$, FDR corrected). In the ADHD group there was only a slight suppression in the theta-alpha band DFAs and a robust increase in the wide gamma-band DFAs) during task compared to RS in both tasks (Fig. 3A). These differences in the task dependent modulations of DFA exponents were significantly different between the groups (Welch's *t*- test, $p < 0.05$, FDR corrected).

The suppression of theta-alpha band DFAs in TSDT task was widespread in the control group but restricted to somatomotor (SM) system in ADHD patients (Fig. 3B). This suggests that, during the performance of sensory detection task, ADHD patients successfully inhibit LRTCs only in the motor system, but not in other brain regions like the control group. In the Go/NoGo

Fig. 3

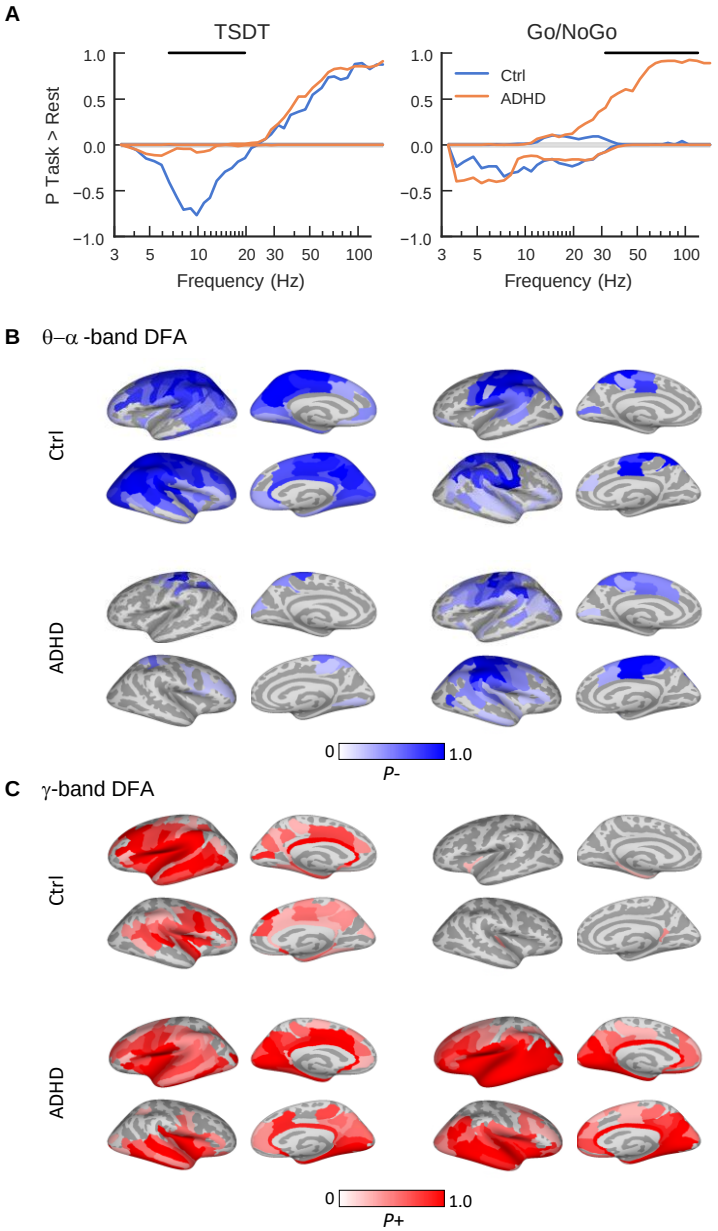

Figure 3. Task dependent modulations of neuronal DFA exponents. (**A**) Differences in DFA exponents between task and rest for control (blue) and ADHD patients (orange) groups (Wilcoxon signed rank test, $p < 0.05$, FDR corrected). The positive values indicate the DFA exponents that were larger for the task than rest and vice versa for the negative values. Axis and shading as in Figure 2D. The black bars above the plot indicate significant differences between the control and ADHD group (Welch *t*-test, $p < 0.05$, FDR corrected). Grey shading displays Q -level of 0.025 for 95th percentile. (**B**) Cortical regions in which the DFA exponents were reduced in theta/alpha (θ-α, 6-13 Hz) by task performance and (**C**) increased in the gamma (γ) band (30-60 Hz). The colors as in Figure 2E.

task, in which successful performance is dependent on inhibition and on the activity of PFC, the suppression of theta-alpha band DFAs was restricted to SM in control group but was also found in the PFC in the ADHD group, pointing to abnormal regulations of LRTCs in the key region underlying task performance (Fig. 3B). In contrast to suppressed theta-alpha DFAs, gamma band DFAs in both tasks were slightly increased during task performance in the control group (Fig. 3A) (Wilcoxon signed rank test, $p < 0.05$, FDR corrected) in visual and PFC regions (Fig. 3C), but robustly increased in ADHD group in nearly all brain regions (Fig. 3C).

Neuronal LRTCs predict LRTCs in behavioral performance

We next tested whether neuronal LRTCs could predict LRTCs in behavioral task performance. Neuronal and behavioral DFAs in the TSDT task showed significant robust positive correlations for ADHD group in alpha and beta bands, which was not seen for the control group (Fig. 4A, Spearman rank correlation, $p < 0.05$, FDR corrected). In the Go/NoGo task behavioral and neuronal DFAs were correlated positively with performance in the control group in the alpha band (Fig. 4A) while in ADHD group there was a negative correlation between theta-alpha band DFAs and task performance. In ADHD patients, these correlations arised from the activity in visual systems (Fig. 4B-C) while in control group positive correlations arised from the PFC.

Neuronal LRTCs correlate with the ADHD symptom scores

Finally, to test whether aberrant LRTCs were clinically relevant, we investigated if LRTCs were correlated with ADHD symptoms as quantified with ASRS and BIS scores. In both tasks, neuronal DFAs in the theta-beta band were negatively correlated with ASRS and BIS scores in ADHD patients (Fig. 5A). This indicated that smaller DFA exponents in patients were found to accompany worse ADHD symptoms in several parcels. In contrast, in healthy participants

Fig. 4

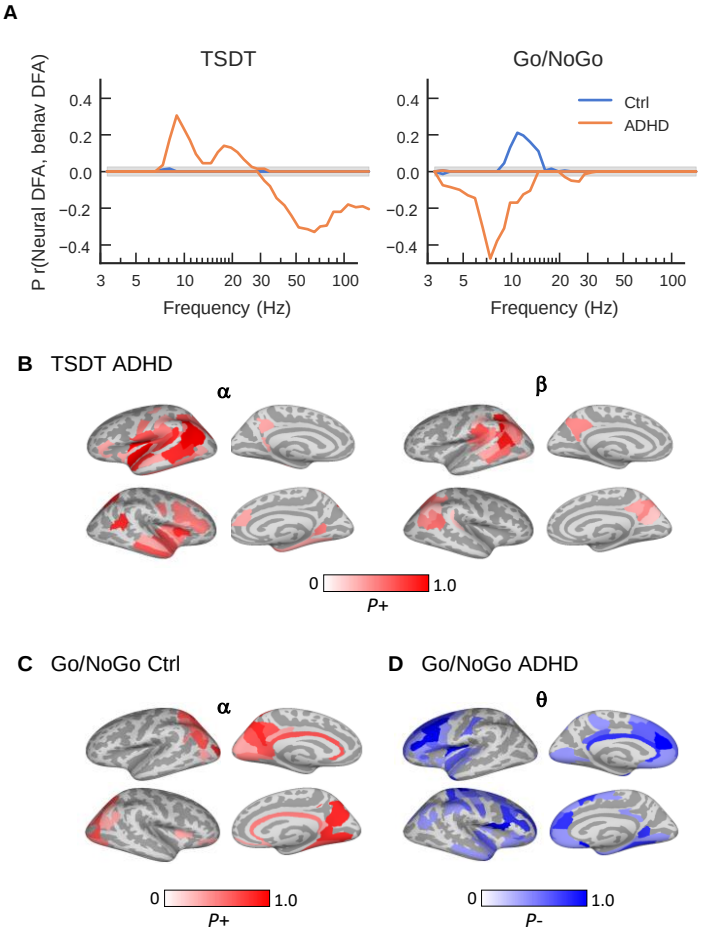

Figure 4. Correlations between the neural and behavioral DFA exponents. (**A**) Group-level correlation of neural and behavioral DFA exponents within subjects for TSDT and Go/NoGo tasks (Spearman-Rank correlation test, $p < 0.05$, FDR corrected). The *y*-axis shows the fraction of cortical parcels (*P*) with significant correlations and grey shading Q-level of 0.025 for 95th percentile (**B**) Cortical regions in which neural DFA exponents were correlated with behavioral LRTCs in ADHD patients in TSDT (Threshold of Stimulus Detection Task) tasks in the alpha (α, 8-13 Hz) and beta (β, 14-30 Hz) bands. **(C)** Cortical regions in which neural DFA exponents were correlated with behavioral LRTCs in the Go/NoGo task in Control subjects in the alpha band, and **(D)** in ADHD subjects in the theta band. Colors as in Figure 3B and 3C.

larger DFA exponents accompanied non-clinical increase in the ASSR and BIS scores (Fig 5B). To further understand this bimodal distribution, we next averaged DFAs over all cortical parcels at a peak correlation frequency of 17 Hz and plotted the correlation of DFA exponents with ASRS and BIS scores (Fig. 5C). Taken the opposite correlations between LRTCs and symptom scores in the healthy controls and ADHD groups, we tested whether the correlations would be explained by an inverted U-shaped curve (*i.e* parabolic) where largest LRTCs are obtained with intermediate symptom score values. To this end, we estimated the partial quadratic correlations by regressing out the linear components between DFA exponents with ASRS and BIS scores. As predicted, quadratic correlations were significant both in TSDT and Go/NoGo tasks, demonstrating that maximal LRTCs values are obtained in the border between neurotypical behavior and ADHD symptoms (Fig. 5C).

Discussion

LRTCs are a characteristic feature of behavioral performance and healthy brain activity[59] while their aberrancies are a characteristic feature of many brain diseases.[37–45] We investigated whether aberrant behavioral fluctuations in sustained tasks in ADHD could arise from aberrant long-range temporal neuronal dynamics. We show here that behavioral LRTCs are decreased in ADHD in Go/NoGo task measuring response inhibition and cognitive control, this being paralleled by aberrant LRTCs of oscillation amplitude fluctuations. The deviant neuronal LRTCs were correlated with inter-individual variability in behavioral LRTCs both in TSDT and Go/NoGo CPTs, suggesting that aberrant neuronal fluctuations can be the cause of aberrant behavioral fluctuations in adult ADHD patients. Overall, these data demonstrate that altered LRTCs in oscillation amplitudes might constitute to the aberrant involuntary fluctuations of attention of adults with ADHD.

Fig. 5

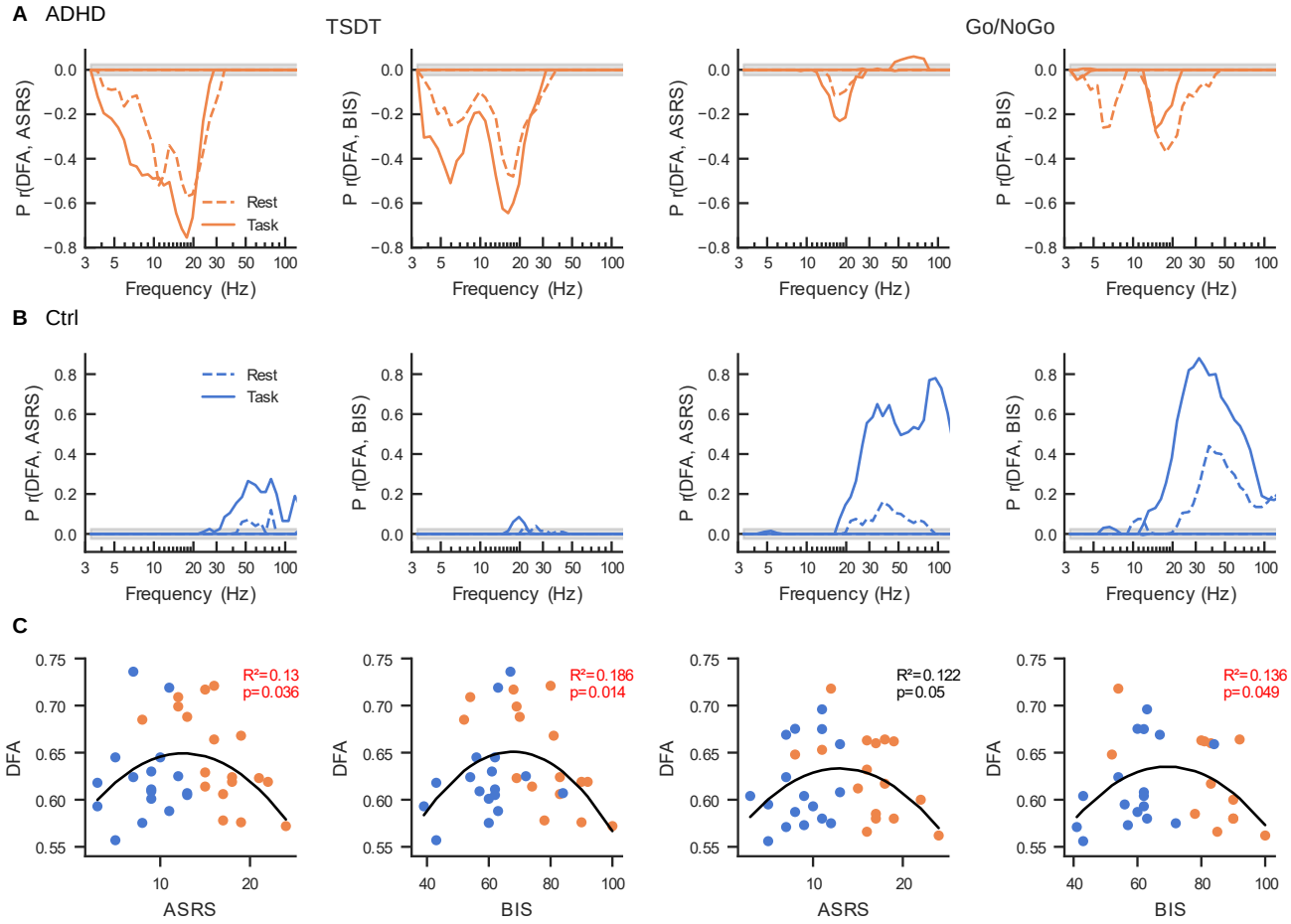

Figure 5. ADHD symptom scores predict neuronal LRTCs with an inverted U-shaped curve. (**A**) Correlation of neuronal DFA values obtained from task data (solid line) and resting state data (dashed line) with total ASR (N = 20) and BIS (N = 18) scores in the ADHD group (Spearman rank correlation test, $p < 0.05$, FDR corrected) for TSDT and Go/NoGo tasks. Grey shading displays Q -level of 0.025 for 95th percentile. (**B**) The same as in A but for the control group. (**C**) Scatter plots of the correlations between 17 Hz DFA and ASRS and BIS scores for for both TSDT and Go/NoGo data.

ADHD patients had aberrant LRTCs in alpha and gamma-band oscillation amplitude fluctuations compared to neurotypical controls, both during resting-state and CPT execution. This shows that in ADHD, oscillation dynamics is altered across time scales from seconds to minutes, in addition to the previously found sub-second time scale abnormalities in alpha band for adult,[21,27,29] adolescent[60,61] and child ADHD patients,[30] and in theta-[62] and gamma-bands for adult ADHD.[20] These results are also in line with a recent study reporting intrinsic temporal variability in functional connectivity in ADHD patients[63] and show that aberrant temporal dynamics is also a characteristic of local neuronal processing. ADHD patients had larger alpha band LRTCs in RS compared control group suggestive of longer periods of mind wandering[64,65] In contrast, while in the control group alpha-band LRTCs were suppressed in task compared to RS-activity, this suppression was not evident in ADHD group. Instead, increased gamma-band LRTCs in the Go/NoGo task compared to RS was only observed in the ADHD group. This differential pattern of alpha and gamma frequency band LRTCs changes in response to task performance suggests that ADHD patients might have developed a compensatory mechanism to overcome the deficits in sustaining attention in experimental conditions.[66] The localization of LRTCs was widespread across cortical regions, in line with prior studies of LRTCs location[14] and results showing that altered neuronal processing in ADHD characterizes multiple brain systems in terms of fMRI BOLD signal strength[67–75] and functional connectivity[16,70,73,76] as well as MEG oscillation power and connectivity[28,77] analyses. DAN (Dorsal Attention Network) hyperactivation and stronger within-network connectivity of both VAN (Ventral Attention Network) and DAN[78] have previously been interpreted as either a compensatory mechanism[79] or deficient segregation of these networks. This implies that ADHD patients are challenged in engaging whichever network is more relevant for current behavioral goals. This supports the idea that increased task-dependent gamma-band LRTCs found in Go/NoGo task for ADHD patients reflect a compensatory mechanism to overcome difficulties in task performance demanding cognitive control. Opposite changes of alpha- and gamma-band LRTCs could lead to the behavioral deficits observed in ADHD, such as the increased attention

to distracting information reflected in stronger ERPs[80] and a tendency for mind wandering[81]. In line with this idea, alpha and beta band LRTCs were correlated with behavioral DFA during task performance in TSDT task more strongly in ADHD patients. This suggest that sensory-driven task differences in LRTCs in oscillation amplitude fluctuations could lead to aberrant behavioral fluctuations observed previously to characterize ADHD.[82] These findings are in line with hypoarousal and unstable vigilance regulation as a possible factor contributing to ADHD symptoms.[83,84]

Importantly, neuronal LRTCs predicted the ASRS and BIS symptom scores with quadratic correlations indicating inverted U-shaped correlations where LRTCs are maximal for intermediate symptom scores in the regime between neurotypical features and mild ADHD symptoms. In contrast, both low symptom scores in control subjects and high symptom scores in ADHD patients were associated with smaller LRTCs. As high LRTCs are the hallmarks of brain criticality,[36] this demonstrates that moderate symptom scores and mild ADHD are associated with the brain operating closer to the critical point. Since, brain criticality is thought to maximize flexible routing of information, storage capacity,[36] and optimal performance in behavioral data,[12] this suggest that moderate ADHD symptoms scores are associated with these optimal brain states and are obtained in neurotypical controls with strong ADHD features and in ADHD patients with mild symptoms. In contrast, neurotypical controls with low ADHD symptom scores and ADHD patients with high symptoms scores were associated with smaller DFA exponents are thought to reflect suboptimal brain dynamics that might be detrimental for behavioral performance, yielding to less flexible information processing and storage capacity. These data constitute evidence that altered LRTCs are not only a core disease mechanism causing ADHD symptoms and behavioral deficits, but also leads to behavioral variability and putatively to personality characteristics in the healthy neurotypical population.

Importantly excitation-inhibition (E/I) (E/I ratio) is the main control parameter of critical dynamics such that it emerges at E/I balance, while excess inhibition or excitation leads to sub-

or super-critical dynamics, respectively[85–91]. In line with this framework, LRTCs are influenced by pharmacological modulations of neuronal excitability[92–95] as well as by polymorphism in neuromodulatory genes[96]. Aberrant LRTCs in ADHD could hence arise via mechanisms that influence the E/I ratio at the systems level or in specific neuronal circuits. Specifically, the norepinephrine (NE) system modulates attentional allocation[97] and NE reuptake inhibitor are used for treatment of ADHD.[98] Modulation of NE levels would therefore be a plausible candidate mechanisms influencing LRTCs. However, taken the inverted U-shaped correlations between the LRTCs and ADHD symptoms, the optimal dose giving rise to maximal LRTCs are likely to grossly vary across individuals.

Acknowledgements

We thank Anna Lampinen for collecting the neuropsychological data.

Funding

This study was supported by funding from the Sigrid Juselius foundation to SP and JMP, Ella and Georg Ehrnrooth Foundation to IMM, and the Academy of Finland (SA 1294761) to JS.

Competing interests

All authors report no biomedical financial interests or potential conflicts of interest.

References

1. Martin J, Hamshere ML, Stergiakouli E, O'Donovan MC, Thapar A. Genetic Risk for Attention-Deficit/Hyperactivity Disorder Contributes to Neurodevelopmental Traits in

the General Population. *Cortical Development in Attention-Deficit/Hyperactivity Disorder*. 2014;76(8):664-671. doi:10.1016/j.biopsych.2014.02.013

2. Taylor MJ, Polderman TJC. Introduction to the Special Issue on 'The Genetic Architecture of Neurodevelopmental Disorders.' *Behav Genet*. 2020;50(4):185-190. doi:10.1007/s10519-020-10007-x

3. Faraone SV, Asherson P, Banaschewski T, et al. Attention-deficit/hyperactivity disorder. *Nature Reviews Disease Primers*. 2015;1(1):15020. doi:10.1038/nrdp.2015.20

4. Lange KW, Hauser J, Lange KM, et al. Utility of cognitive neuropsychological assessment in attention-deficit/hyperactivity disorder. *ADHD Attention Deficit and Hyperactivity Disorders*. 2014;6(4):241-248. doi:10.1007/s12402-014-0132-3

5. Uddin LQ, Dajani DR, Voorhies W, Bednarz H, Kana RK. Progress and roadblocks in the search for brain-based biomarkers of autism and attention-deficit/hyperactivity disorder. *Translational Psychiatry*. 2017;7(8):e1218-e1218. doi:10.1038/tp.2017.164

6. Kofler MJ, Rapport MD, Sarver DE, et al. Reaction time variability in ADHD: a meta-analytic review of 319 studies. *ClinPsycholRev*. 2013;33(6):795-811.

7. Gilden DL, Hancock H. Response variability in attention-deficit disorders. *PsycholSci*. 2007;18(9):796-802. doi:10.1111/j.1467-9280.2007.01982.x

8. Castellanos FX, Tannock R. Neuroscience of attention-deficit/hyperactivity disorder: the search for endophenotypes. *NatRevNeurosci*. 2002;3(8):617-628. doi:10.1038/nrn896

9. Klein C, Wendling K, Huettner P, Ruder H, Peper M. Intra-Subject Variability in Attention-Deficit Hyperactivity Disorder. *Biological Psychiatry*. 2006;60(10):1088-1097. doi:10.1016/j.biopsych.2006.04.003

10. Levy F, Pipingas A, Harris EV, Farrow M, Silberstein RB. Continuous performance task in ADHD: Is reaction time variability a key measure? *NeuropsychiatrDisTreat*. 2018;14(Journal Article):781-786. doi:10.2147/NDT.S158308

11. Monto S, Palva S, Voipio J, Palva JM. Very slow EEG fluctuations predict the dynamics of stimulus detection and oscillation amplitudes in humans. *JNeurosci*. 2008;28(33):8268-8272. doi:10.1523/JNEUROSCI.1910-08.2008

12. Simola J, Zhigalov A, Morales-Munoz I, Palva JM, Palva S. Critical dynamics of endogenous fluctuations predict cognitive flexibility in the Go/NoGo task. *SciRep*. 2017;7(1):2909-017-02750-02759. doi:10.1038/s41598-017-02750-9

13. Stuss DT, Murphy KJ, Binns MA, Alexander MP. Staying on the job: the frontal lobes control individual performance variability. *Brain*. 2003;126(Pt 11):2363-2380. doi:10.1093/brain/awg237

14. Palva JM, Zhigalov A, Hirvonen J, Korhonen O, Linkenkaer-Hansen K, Palva S. Neuronal long-range temporal correlations and avalanche dynamics are correlated with behavioral scaling laws. *ProcNatlAcadSciUSA*. 2013;110(9):3585-3590. doi:10.1073/pnas.1216855110

15. Hoogman M, Bralten J, Hibar DP, et al. Subcortical brain volume differences in participants with attention deficit hyperactivity disorder in children and adults: a cross-

sectional mega-analysis. *Lancet Psychiatry*. 2017;4(4):310-319. doi:10.1016/S2215-0366(17)30049-4

16. Konrad K, Eickhoff SB. Is the ADHD brain wired differently? A review on structural and functional connectivity in attention deficit hyperactivity disorder. *Hum Brain Mapp*. 2010;31(6):904-916. doi:10.1002/hbm.21058

17. Samea F, Soluki S, Nejati V, et al. Brain alterations in children/adolescents with ADHD revisited: A neuroimaging meta-analysis of 96 structural and functional studies. *Neurosci Biobehav Rev*. 2019;100:1-8. doi:10.1016/j.neubiorev.2019.02.011

18. Bellato A, Norman L, Idrees I, et al. A systematic review and meta-analysis of altered electrophysiological markers of performance monitoring in Obsessive-Compulsive Disorder (OCD), Gilles de la Tourette Syndrome (GTS), Attention-Deficit/Hyperactivity disorder (ADHD) and Autism. *NeurosciBiobehavRev*. 2021;131(Journal Article):964-987.

19. Lenartowicz A, Mazaheri A, Jensen O, Loo SK. Aberrant Modulation of Brain Oscillatory Activity and Attentional Impairment in Attention-Deficit/Hyperactivity Disorder. *BiolPsychiatryCognNeurosciNeuroimaging*. 2018;3(1):19-29.

20. Dor-Ziderman Y, Zeev-Wolf M, Hirsch Klein E, et al. High-gamma oscillations as neurocorrelates of ADHD: A MEG crossover placebo-controlled study. *JPsychiatrRes*. 2021;137(Journal Article):186-193.

21. Michelini G, Salmastyan G, Vera JD, Lenartowicz A. Event-related brain oscillations in attention-deficit/hyperactivity disorder (ADHD): A systematic review and meta-analysis. *International Journal of Psychophysiology*. 2022;174:29-42. doi:10.1016/j.ijpsycho.2022.01.014

22. Klimesch W, Sauseng P, Hanslmayr S. EEG alpha oscillations: the inhibition-timing hypothesis. *Brain ResRev*. 2007;53(1):63-88. doi:10.1016/j.brainresrev.2006.06.003

23. Palva S, Palva JM. New vistas for alpha-frequency band oscillations. *Trends Neurosci*. 2007;30(4):150-158. doi:10.1016/j.tins.2007.02.001

24. Thut G, Miniussi C, Gross J. The functional importance of rhythmic activity in the brain. *CurrBiol*. 2012;22(16):R658-63. doi:10.1016/j.cub.2012.06.061

25. Jensen O, Bonnefond M, Marshall TR, Tiesinga P. Oscillatory mechanisms of feedforward and feedback visual processing. *Trends Neurosci*. 2015;38(4):192-194. doi:10.1016/j.tins.2015.02.006

26. Urbain C, Vogan VM, Ye AX, Pang EW, Doesburg SM, Taylor MJ. Desynchronization of fronto-temporal networks during working memory processing in autism. *Human Brain Mapping*. 2016;37(1):153-164. doi:10.1002/hbm.23021

27. Hasler R, Perroud N, Meziane HB, et al. Attention-related EEG markers in adult ADHD. *Neuropsychologia*. 2016;87(Journal Article):120-133. doi:10.1016/j.neuropsychologia.2016.05.008

28. Mazzetti C, Gonzales Damatac C, Sprooten E, Ter Huurne N, Buitelaar JK, Jensen O. Dorsal-to-ventral imbalance in the superior longitudinal fasciculus mediates

methylphenidate's effect on beta oscillations in ADHD. *Psychophysiology*. Published online February 14, 2022:e14008. doi:10.1111/psyp.14008

29. ter Huurne N, Onnink M, Kan C, Franke B, Buitelaar J, Jensen O. Behavioral Consequences of Aberrant Alpha Lateralization in Attention-Deficit/Hyperactivity Disorder. *Oxytocin and Autism*. 2013;74(3):227-233. doi:10.1016/j.biopsych.2013.02.001

30. Vollebregt MA, Zumer JM, Ter Huurne N, Buitelaar JK, Jensen O. Posterior alpha oscillations reflect attentional problems in boys with Attention Deficit Hyperactivity Disorder. *ClinNeurophysiol*. 2016;127(5):2182-2191. doi:10.1016/j.clinph.2016.01.021

31. Linkenkaer-Hansen K, Nikouline VV, Palva JM, Ilmoniemi RJ. Long-range temporal correlations and scaling behavior in human brain oscillations. *JNeurosci*. 2001;21(4):1370-1377.

32. Zhigalov A, Arnulfo G, Nobili L, Palva S, Palva JM. Modular co-organization of functional connectivity and scale-free dynamics in the human brain. *Network Neuroscience*. 2017;1(2):143-165. doi:10.1162/NETN_a_00008

33. Smit DJ, Linkenkaer-Hansen K, de Geus EJ. Long-range temporal correlations in resting-state alpha oscillations predict human timing-error dynamics. *JNeurosci*. 2013;33(27):11212-11220. doi:10.1523/JNEUROSCI.2816-12.2013

34. Thiery T, Lajnef T, Combrisson E, et al. Long-range temporal correlations in the brain distinguish conscious wakefulness from induced unconsciousness. *Neuroimage*. 2018;179(Journal Article):30-39.

35. Zhigalov A, Arnulfo G, Nobili L, Palva S, Palva JM. Relationship of Fast- and Slow-Timescale Neuronal Dynamics in Human MEG and SEEG. *JNeurosci*. 2015;35(13):5385-5396. doi:10.1523/JNEUROSCI.4880-14.2015

36. Cocchi L, Gollo LL, Zalesky A, Breakspear M. Criticality in the brain: A synthesis of neurobiology, models and cognition. *ProgNeurobiol*. 2017;(Journal Article).

37. Monto S, Vanhatalo S, Holmes MD, Palva JM. Epileptogenic Neocortical Networks Are Revealed by Abnormal Temporal Dynamics in Seizure-Free Subdural EEG. *Cerebral Cortex*. 2007;17(6):1386-1393. doi:10.1093/cercor/bhl049

38. Montez T, Poil SS, Jones BF, et al. Altered temporal correlations in parietal alpha and prefrontal theta oscillations in early-stage Alzheimer disease. *ProcNatlAcadSciUSA*. 2009;106(5):1614-1619. doi:10.1073/pnas.0811699106

39. Nikulin VV, Jonsson EG, Brismar T. Attenuation of long-range temporal correlations in the amplitude dynamics of alpha and beta neuronal oscillations in patients with schizophrenia. *Neuroimage*. 2012;61(1):162-169. doi:10.1016/j.neuroimage.2012.03.008

40. Moran JK, Michail G, Heinz A, Keil J, Senkowski D. Long-Range Temporal Correlations in Resting State Beta Oscillations are Reduced in Schizophrenia. *FrontPsychiatry*. 2019;10(Journal Article):517. doi:10.3389/fpsyt.2019.00517

41. Cruz G, Grent-'t-Jong T, Krishnadas R, Palva JM, Palva S, Uhlhaas PJ. Long range temporal correlations (LRTCs) in MEG-data during emerging psychosis: Relationship

to symptoms, medication-status and clinical trajectory. *Neuroimage Clin*. 2021;31(Journal Article):102722.

42. Damiani S, Scalabrini A, Gomez-Pilar J, Brondino N, Northoff G. Increased scale-free dynamics in salience network in adult high-functioning autism. *Neuroimage Clin*. 2019;21(Journal Article):101634.

43. Jia H, Yu D. Attenuated long-range temporal correlations of electrocortical oscillations in patients with autism spectrum disorder. *DevCognNeurosci*. 2019;39(Journal Article):100687.

44. Linkenkaer-Hansen K, Monto S, Rytsala H, Suominen K, Isometsa E, Kahkonen S. Breakdown of long-range temporal correlations in theta oscillations in patients with major depressive disorder. *JNeurosci*. 2005;25(44):10131-10137. doi:10.1523/JNEUROSCI.3244-05.2005

45. Duncan NW, Hsu TY, Cheng PZ, Wang HY, Lee HC, Lane TJ. Intrinsic activity temporal structure reactivity to behavioural state change is correlated with depressive symptoms. *EurJNeurosci*. 2020;(Journal Article). doi:10.1111/ejn.14858

46. Cowley B, Holmström É, Juurmaa K, Kovarskis L, Krause CM. Computer Enabled Neuroplasticity Treatment: A Clinical Trial of a Novel Design for Neurofeedback Therapy in Adult ADHD. *FrontHumNeurosci*. 2016;10(Journal Article):205. doi:10.3389/fnhum.2016.00205

47. Patton JH, Stanford MS, Barratt ES. Factor structure of the Barratt impulsiveness scale. *JClinPsychol*. 1995;51(6):768-774. doi:10.1002/1097-4679(199511)51:6<768::aid-jclp2270510607>3.0.co;2-1

48. Davenport T L, Davis AS. Brown Attention-Deficit Disorder Scales. In: Goldstein S, Naglieri JA, eds. *Encyclopedia of Child Behavior and Development*. Springer US; 2011:302-303. doi:10.1007/978-0-387-79061-9_439

49. Kessler RC, Adler L, Ames M, et al. The World Health Organization Adult ADHD Self-Report Scale (ASRS): a short screening scale for use in the general population. *PsycholMed*. 2005;35(2):245-256. doi:10.1017/s0033291704002892

50. Watson AB, Pelli DG. QUEST: A Bayesian adaptive psychometric method. *PerceptPsychophys*. 1983;33(2):113-120.

51. Perlin K. An Image Synthesizer. *SIGGRAPH ComputGraph*. 1985;19(3):287-296. doi:10.1145/325165.325247

52. Hardstone R, Poil SS, Schiavone G, et al. Detrended fluctuation analysis: a scale-free view on neuronal oscillations. *FrontPhysiol*. 2012;3(Journal Article):450. doi:10.3389/fphys.2012.00450;

53. Lobier M, Palva JM, Palva S. High-alpha band synchronization across frontal, parietal and visual cortex mediates behavioral and neuronal effects of visuospatial attention. *Neuroimage*. 2017;165(Journal Article):222-237.

54. Hirvonen J, Monto S, Wang S, Palva J, Palva S. Dynamic large-scale network synchronization from perception to action. *Network Neuroscience*. 2018;2(4):442-463. doi:10.1162/netn_a_00039

55. Siebenhühner F, Wang SH, Arnulfo G, Nobili L, Palva JM, Palva S. Resting-state cross-frequency coupling networks in human electrophysiological recordings. *bioRxiv (preprint)*. 2019;(Journal Article):547638. doi:10.1101/547638

56. Gramfort A, Luessi M, Larson E, et al. MNE software for processing MEG and EEG data. *Neuroimage*. 2014;86(Journal Article):446-460. doi:10.1016/j.neuroimage.2013.10.027

57. Korhonen O, Palva S, Palva JM. Sparse weightings for collapsing inverse solutions to cortical parcellations optimize M/EEG source reconstruction accuracy. *JNeurosciMethods*. 2014;226C(Journal Article):147-160. doi:10.1016/j.jneumeth.2014.01.031

58. Stanford MS, Mathias CW, Dougherty DM, Lake SL, Anderson NE, Patton JH. Fifty years of the Barratt Impulsiveness Scale: An update and review. *Personality and Individual Differences*. 2009;47(5):385-395. doi:10.1016/j.paid.2009.04.008

59. Palva S, Palva JM. Roles of brain criticality and multiscale oscillations in sensorimotor predictions. *Trends Neurosci*. 2018;41(10):729-743,. doi:10.1016/j.tins.2018.08.008

60. Mazaheri A, Fassbender C, Coffey-Corina S, Hartanto TA, Schweitzer JB, Mangun GR. Differential oscillatory electroencephalogram between attention-deficit/hyperactivity disorder subtypes and typically developing adolescents. *BiolPsychiatry*. 2014;76(5):422-429. doi:10.1016/j.biopsych.2013.08.023

61. Debnath R, Miller NV, Morales S, Seddio KR, Fox NA. Investigating brain electrical activity and functional connectivity in adolescents with clinically elevated levels of ADHD symptoms in alpha frequency band. *Brain Res*. 2021;1750(Journal Article):147142.

62. Cowley BU, Juurmaa K, Palomäki J. Reduced Power in Fronto-Parietal Theta EEG Linked to Impaired Attention-Sampling in Adult ADHD. *eNeuro*. 2022;9(1). doi:10.1523/ENEURO.0028-21.2021

63. Barttfeld P, Petroni A, Báez S, et al. Functional Connectivity and Temporal Variability of Brain Connections in Adults with Attention Deficit/Hyperactivity Disorder and Bipolar Disorder. *Neuropsychobiology*. 2014;69(2):65-75. doi:10.1159/000356964

64. Kam JWY, Rahnuma T, Park YE, Hart CM. Electrophysiological markers of mind wandering: A systematic review. *Neuroimage*. 2022;258:119372. doi:10.1016/j.neuroimage.2022.119372

65. Jin CY, Borst JP, van Vugt MK. Predicting task-general mind-wandering with EEG. *Cogn Affect Behav Neurosci*. 2019;19(4):1059-1073. doi:10.3758/s13415-019-00707-1

66. Sonuga-Barke E, Bitsakou P, Thompson M. Beyond the dual pathway model: evidence for the dissociation of timing, inhibitory, and delay-related impairments in attention-deficit/hyperactivity disorder. *JAmAcadChild AdolescPsychiatry*. 2010;49(4):345-355.

67. Rubia K, Alegria A, Brinson H. Imaging the ADHD brain: disorder-specificity, medication effects and clinical translation. *Expert RevNeurother*. 2014;14(5):519-538. doi:10.1586/14737175.2014.907526

68. Cubillo A, Halari R, Smith A, Taylor E, Rubia K. A review of fronto-striatal and fronto-cortical brain abnormalities in children and adults with Attention Deficit Hyperactivity Disorder (ADHD) and new evidence for dysfunction in adults with ADHD during motivation and attention. *Cortex*. 2012;48(2):194-215. doi:10.1016/j.cortex.2011.04.007

69. Bush G. Cingulate, Frontal, and Parietal Cortical Dysfunction in Attention-Deficit/Hyperactivity Disorder. *Prefrontal Cortical Circuits Regulating Attention, Behavior and Emotion*. 2011;69(12):1160-1167. doi:10.1016/j.biopsych.2011.01.022

70. Bush G. Attention-Deficit/Hyperactivity Disorder and Attention Networks. *Neuropsychopharmacology*. 2010;35(1):278-300. doi:10.1038/npp.2009.120

71. Cortese S, Kelly C, Chabernaud C, et al. Toward Systems Neuroscience of ADHD: A Meta-Analysis of 55 fMRI Studies. *AmJPsychiatry*. 2012;169(10):1038-1055. doi:10.1176/appi.ajp.2012.11101521

72. Hart H, Radua J, Mataix-Cols D, Rubia K. Meta-analysis of fMRI studies of timing in attention-deficit hyperactivity disorder (ADHD). *Neuroscience & Biobehavioral Reviews*. 2012;36(10):2248-2256. doi:10.1016/j.neubiorev.2012.08.003

73. Dickstein SG, Bannon K, Castellanos FX, Milham MP. The neural correlates of attention deficit hyperactivity disorder: an ALE meta-analysis. *JChild PsycholPsychiatry*. 2006;47(10):1051-1062.

74. Castellanos FX, Proal E. Large-scale brain systems in ADHD: beyond the prefrontal–striatal model. *Special Issue: Cognition in Neuropsychiatric Disorders*. 2012;16(1):17-26. doi:10.1016/j.tics.2011.11.007

75. Cao M, Shu N, Cao Q, Wang Y, He Y. Imaging Functional and Structural Brain Connectomics in Attention-Deficit/Hyperactivity Disorder. *MolNeurobiol*. 2014;50(3):1111-1123. doi:10.1007/s12035-014-8685-x

76. De La Fuente A, Xia S, Branch C, Li X. A review of attention-deficit/hyperactivity disorder from the perspective of brain networks. *Frontiers in Human Neuroscience*. 2013;7(Journal Article):192.

77. Vandewouw MM, Dunkley BT, Lerch JP, Anagnostou E, Taylor MJ. Characterizing Inscapes and resting-state in MEG: Effects in typical and atypical development. *Neuroimage*. 2021;225:117524. doi:10.1016/j.neuroimage.2020.117524

78. Sidlauskaite J, Sonuga-Barke E, Roeyers H, Wiersema JR. Altered intrinsic organisation of brain networks implicated in attentional processes in adult attention-deficit/hyperactivity disorder: a resting-state study of attention, default mode and salience network connectivity. *EurArchPsychiatry ClinNeurosci*. 2016;266(4):349-357. doi:10.1007/s00406-015-0630-0

79. Thomason ME, Chang CE, Glover GH, Gabrieli JD, Greicius MD, Gotlib IH. Default-mode function and task-induced deactivation have overlapping brain substrates in children. *Neuroimage*. 2008;41(4):1493-1503. doi:10.1016/j.neuroimage.2008.03.029

80. Prox V, Dietrich DE, Zhang Y, Emrich HM, Ohlmeier MD. Attentional processing in adults with ADHD as reflected by event-related potentials. *NeurosciLett*. 2007;419(3):236-241.

81. Bozhilova NS, Michelini G, Kuntsi J, Asherson P. Mind wandering perspective on attention-deficit/hyperactivity disorder. *NeurosciBiobehavRev*. 2018;92(Journal Article):464-476.

82. Castellanos FX, Sonuga-Barke EJ, Scheres A, Di Martino A, Hyde C, Walters JR. Varieties of attention-deficit/hyperactivity disorder-related intra-individual variability. *BiolPsychiatry*. 2005;57(11):1416-1423. doi:10.1016/j.biopsych.2004.12.005

83. Hegerl U, Hensch T. The vigilance regulation model of affective disorders and ADHD. *Neuroscience & Biobehavioral Reviews*. 2014;44:45-57. doi:10.1016/j.neubiorev.2012.10.008

84. Martella D, Aldunate N, Fuentes LJ, Sánchez-Pérez N. Arousal and Executive Alterations in Attention Deficit Hyperactivity Disorder (ADHD). *Frontiers in Psychology*. 2020;11. Accessed January 27, 2022. https://www.frontiersin.org/article/10.3389/fpsyg.2020.01991

85. Poil SS, Hardstone R, Mansvelder HD, Linkenkaer-Hansen K. Critical-State Dynamics of Avalanches and Oscillations Jointly Emerge from Balanced Excitation/Inhibition in Neuronal Networks. *JNeurosci*. 2012;32(Journal Article):9817-9823.

86. Shew WL, Yang H, Petermann T, Roy R, Plenz D. Neuronal avalanches imply maximum dynamic range in cortical networks at criticality. *JNeurosci*. 2009;29(49):15595-15600. doi:10.1523/JNEUROSCI.3864-09.2009

87. Bruining H, Hardstone R, Juarez-Martinez EL, et al. Measurement of excitation-inhibition ratio in autism spectrum disorder using critical brain dynamics. *SciRep*. 2020;10(1):9195-020-65500-65504. doi:10.1038/s41598-020-65500-4

88. Rubinov M, Sporns O, Thivierge JP, Breakspear M. Neurobiologically realistic determinants of self-organized criticality in networks of spiking neurons. *PLoS ComputBiol*. 2011;7(6):e1002038. doi:10.1371/journal.pcbi.1002038

89. Liang J, Zhou T, Zhou C. Hopf Bifurcation in Mean Field Explains Critical Avalanches in Excitation-Inhibition Balanced Neuronal Networks: A Mechanism for Multiscale Variability. *FrontSystNeurosci*. 2020;14(Journal Article):580011. doi:10.3389/fnsys.2020.580011

90. Li J, Shew WL. Tuning network dynamics from criticality to an asynchronous state. *PLoS ComputBiol*. 2020;16(9):e1008268. doi:10.1371/journal.pcbi.1008268

91. Plenz D, Thiagarajan TC. The organizing principles of neuronal avalanches: cell assemblies in the cortex? *Trends Neurosci*. 2007;30(3):101-110. doi:10.1016/j.tins.2007.01.005

92. Stewart CV, Plenz D. Inverted-U profile of dopamine-NMDA-mediated spontaneous avalanche recurrence in superficial layers of rat prefrontal cortex. *JNeurosci*. 2006;26(31):8148-8159. doi:10.1523/JNEUROSCI.0723-06.2006

93. Gireesh ED, Plenz D. Neuronal avalanches organize as nested theta- and beta/gamma-oscillations during development of cortical layer 2/3. *ProcNatlAcadSciUSA*. 2008;105(21):7576-7581. doi:10.1073/pnas.0800537105

94. Pasquale V, Massobrio P, Bologna LL, Chiappalone M, Martinoia S. Self-organization and neuronal avalanches in networks of dissociated cortical neurons. *Neuroscience*. 2008;153(4):1354-1369. doi:10.1016/j.neuroscience.2008.03.050

95. Atasoy S, Roseman L, Kaelen M, Kringelbach ML, Deco G, Carhart-Harris RL. Connectome-harmonic decomposition of human brain activity reveals dynamical repertoire re-organization under LSD. *Sci Rep*. 2017;7(1):17661. doi:10.1038/s41598-017-17546-0

96. Simola J, Siebenhühner F, Myrov V, et al. Genetic polymorphisms in COMT and BDNF influence synchronization dynamics of human neuronal oscillations. *iScience*. 2022;25(9):104985. doi:10.1016/j.isci.2022.104985

97. del Campo N, Fryer TD, Hong YT, et al. A positron emission tomography study of nigro-striatal dopaminergic mechanisms underlying attention: implications for ADHD and its treatment. *Brain*. 2013;136(11):3252-3270. doi:10.1093/brain/awt263

98. Fu D, Wu DD, Guo HL, et al. The Mechanism, Clinical Efficacy, Safety, and Dosage Regimen of Atomoxetine for ADHD Therapy in Children: A Narrative Review. *Front Psychiatry*. 2021;12:780921. doi:10.3389/fpsyt.2021.780921

99. Levina A, Herrmann JM, Geisel T. Theoretical Neuroscience of Self-Organized Criticality: From Formal Approaches to Realistic Models. In: *Criticality in Neural Systems*. John Wiley & Sons, Ltd; 2014:417-436. doi:10.1002/9783527651009.ch20

Figure legends

Figure 1. Task schematics and behavioral data. Schematics of (**A**) Threshold of Stimulus Detection Task (TSDT) and (**B**) Go/NoGo task experiments. (**C**) A short snapshot period of Hit-Miss time-series of a representative subject in TSDT. (**D**) Reaction Time (RT) series of a representative subject for each trial in Go/NoGo. Circles in the lower line above the time-series represent commission errors and circles in the upper line are trials with successful inhibition. (**E**) Distribution of BIS and ASRS scores for N = 21 ADHD patients (orange) and N = 23 neurotypical control (blue) subjects. (**F**) Distribution of Hit rate (HR), and RT distributions separately for TSDT and Go/NoGo tasks. (**G**) False Alarm (FA) rate and Reaction Time Variability (RTV). (**H**) Behavioral DFA (Detrended Fluctuation Analysis) exponents for a representative subject (top) and for the Ctrl and ADHD groups (bottom). Figure displays subject means ± 25 % for each psychophysical parameter. The parenthesis above the figure

illustrates significant difference between the groups for the RTs (two-tailed Mann-Whitney U-test (U = 132), $p = 0.043$)) and RTVs (two-tailed Mann-Whitney U-test, $p = 0.012$).

Figure 2. Differential modulations of neuronal DFA exponents in ADHD and control groups at the whole-brain level. (**A**) Example of unfiltered neuronal time-series (top) and filtered oscillation amplitude time-series (bottom, gray trace) with the amplitude envelope (bottom, black trace) (**B**) DFA exponents extracted from oscillation amplitude envelope for a representative subject. (**C**) Group-level mean DFA -exponents averaged over all parcels as a function of frequency for ADHD (orange) and control (blue) groups during TSDT (Threshold of Stimulus Detection Task) and Go/NoGo tasks. Lines above indicate significant differences between the groups. Gray shading shows 95% confidence intervals. (**D**) Group-level differences in the DFA exponents between control and ADHD groups estimated separately for each cortical parcel (Welch *t*-test, $p < 0.05$, FDR corrected). The *y*-axis shows the fraction of cortical parcels (*P*) in which the difference was significant. Grey lines indicate Q -level of 0.025 for 95th percentile for FDR correction indicating the proportion that could arise by change. (**E**) Cortical regions in which the differences in theta/alpha (θ-α, 6-13 Hz) were observed in TSDT and in theta (θ) -band (5-8 Hz) DFA exponents were observed. The blue color indicates the fraction of time-frequency elements (*P*-) that were significantly suppressed and red the fraction of time-frequency elements (*P*+) that were significantly increased.

Figure 3. Task dependent modulations of neuronal DFA exponents. (**A**) Differences in DFA exponents between task and rest for control (blue) and ADHD patients (orange) groups (Wilcoxon signed rank test, $p < 0.05$, FDR corrected). The positive values indicate the DFA exponents that were larger for the task than rest and vice versa for the negative values. Axis and shading as in Figure 2D. The black bars above the plot indicate significant differences

between the control and ADHD group (Welch *t*-test, $p < 0.05$, FDR corrected). Grey shading displays Q -level of 0.025 for 95th percentile. (**B**) Cortical regions in which the DFA exponents were reduced in theta/alpha (θ-α, 6-13 Hz) by task performance and (**C**) increased in the gamma (γ) band (30-60 Hz). The colors as in Figure 2E.

Figure 4. Correlations between the neural and behavioral DFA exponents. (**A**) Group-level correlation of neural and behavioral DFA exponents within subjects for TSDT and Go/NoGo tasks (Spearman-Rank correlation test, $p < 0.05$, FDR corrected). The *y*-axis shows the fraction of cortical parcels (*P*) with significant correlations and grey shading Q-level of 0.025 for 95th percentile (**B**) Cortical regions in which neural DFA exponents were correlated with behavioral LRTCs in ADHD patients in TSDT (Threshold of Stimulus Detection Task) tasks in the alpha (α, 8-13 Hz) and beta (β, 14-30 Hz) bands. **(C)** Cortical regions in which neural DFA exponents were correlated with behavioral LRTCs in the Go/NoGo task in Control subjects in the alpha band, and **(D)** in ADHD subjects in the theta band. Colors as in Figure 3B and 3C.

Figure 5. ADHD symptom scores predict neuronal LRTCs with an inverted U-shaped curve. (**A**) Correlation of neuronal DFA values obtained from task data (solid line) and resting state data (dashed line) with total ASR (N = 20) and BIS (N = 18) scores in the ADHD group (Spearman rank correlation test, $p < 0.05$, FDR corrected) for TSDT and Go/NoGo tasks. Grey shading displays Q -level of 0.025 for 95th percentile. (**B**) The same as in A but for the control group. (**C**) Scatter plots of the correlations between 17 Hz DFA and ASRS and BIS scores for for both TSDT and Go/NoGo data.